Journal of Materials Chemistry A

Accepted Manuscript

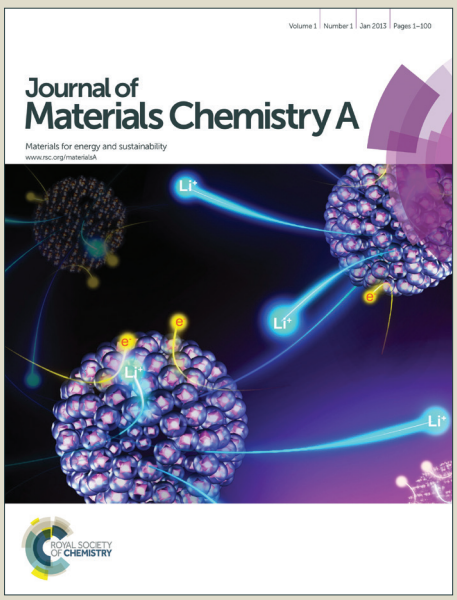

ROYAL SOCIETY OF CHEMISTRY

www.rsc.org/materialsA

Journal of Materials Chemistry A RSCPublishing

ARTICLE

From Chloro to Fluoro, Expanding the Role of Aluminum Phthalocyanine in Organic Photovoltaic Devices

Cite this: DOI: 10.1039/xoxxoooooox

Received ooth January 2012,
Accepted ooth January 2012

DOI: 10.1039/xoxxoooooox

www.rsc.org/

Benoît H. Lessard,[a] Mohammad Al-Amar,[a] Trevor M. Grant,[a] Robin White,[b] Zheng-Hong Lu [b] and Timothy P. Bender*[,a,b,c]

Fluoro aluminum phthalocyanine (F-AlPc) was synthesized by simply heating a DMSO solution of chloro aluminum phthalocyanine (Cl-AlPc) in the presence of CsF, KF or NaF for less than an hour. The resulting F-AlPc has a significant blue shift in the absorbance of ≈ 8 nm in solution and ≈ 130 nm in a solid film compared to Cl-AlPc. Ultraviolet photoelectron spectroscopy (UPS) identified a change in work function and E_{HOMO} of as much as 1 eV between Cl-AlPc and F-AlPc. Our observed change in UPS data, solid-state absorbance and sublimation temperature for F-AlPc further confirms the stacked fluorine bridge solid-state structure for F-AlPc previously described by Kenney et al. Preliminary planar heterojunction (PHJ) organic photovoltaic (OPV) devices were then fabricated using F-AlPc as an electron donating material paired with C_{60} and a ternary device including a Cl-AlPc interlayer. Additionally an all AlPc device where F-AlPc functioned as the electron donor and Cl-AlPc as the electron acceptor was fabricated. The EQE plots of the resulting PHJ OPV devices illustrate that an exciton-rectifying layer is present between the Cl-AlPc and F-AlPc layers in the ternary devices as well as the all AlPc device. These results further exemplify that the seemingly minor change from chloride to fluoride in the AlPc structure has significant implications in optoelectronic properties and functionality of AlPc in PHJ OPV devices.

Introduction

Phthalocyanines (Pcs) are a family of aromatic macrocyclic compounds that can contain a variety of divalent, trivalent or even tetravalent metals.[1] Metal containing Pcs have been utilized in a plethora of applications ranging from pigments/dyes,[1,2] to active materials in organic electronics.[3,4] While the majority of organic electronic examples utilize the divalent metal containing Pcs such as copper Pc (CuPc), a growing interest in trivalent metal containing Pcs has emerged. For example, chloro aluminum Pc (Cl-AlPc) has been paired with C_{60} for the fabrication of a planar heterojunction (PHJ) and blended organic photovoltaic (OPV) devices.[5-9] Cl-AlPc has also been used as an interlayer between PEDOT:PSS and a blended solution of poly(3,3"-didodecylquaterthiophene) (PQT-12) and [6,6]- phenyl-C_{61}-butyric acid methyl ester ($PC_{61}BM$) to form a bilayer bulk heterojunction OPV device.[10]

Our group has recently been studying the incorporation of fluorine groups into boron subphthalocyanine (a sub-class of Pcs) which resulted in a decreases in sublimation temperature, a change in the solid-state arrangement (crystal structure) and a change in electrochemical properties.[11-14] Moving one level down on the periodic table, and given the successful use of Cl-AlPc in OPV devices[5-8] we decided to look at the effect of substituting the axial chloride of Cl-AlPc with a fluoride and incorporate fluoro aluminum Pc (F-AlPc) into simple PHJ OPV devices. In this short paper we outline the results of this effort.

In the early 1980's Kenney and co-workers first reported the synthesis and characterization of F-AlPc (and fluoro gallium Pc (F-GaPc)).[15-17] Through anecdotal observations and by using powder X-ray diffraction Linsky et al. asserted that similar to F-GaPc, F-AlPc has a unique solid-state arrangement where the AlPc fragments are vertically aligned in a unique linear stack with a distance of 3.66Å between AlPcs fragments with the fluorine/fluoride atom equally spaced and interdigitated between the AlPc fragments (**Figure 1**). Following this study, Djurado et al. identified using solid state ^{13}C cross-polarization magic angle spinning (CPMAS) NMR spectroscopy that the Pcs of this stacked F-AlPc were eclipsed in the solid state.[18] While these structures are not polymers, the authors as well as others[18,19] have used this term to describe the linear highly directional, polymeric-like structures. Single crystal X-ray crystallography has been performed on a crystal of Cl-AlPc (identifier code: CUWPAL), however no such results have been reported for F-AlPc. The known single crystal of Cl-AlPc contains a significant amount of disorder (void volume 52%) but it does have a portion that is translationally ordered and therefore has a markedly different solid state arrangement than the stacked structure of F-AlPc (**Figure 1**).[18,20] During the mid-1980s to the mid-1990s, additional researchers found that the unique F-AlPc structure was amenable to chemical doping for increasing its conductivity.[21-24] It was also

found that F-AlPc would outperform other MPcs such as copper phthaolocyanine (CuPc) when used as a conductive matrix for gas sensing applications of NO_2, O_2 and even Cl_2.[25-27] Since this time little to no studies of F-AlPc have appeared in the literature.

In all these cases, the synthesis of F-AlPc was reported using a two-step process where Cl-AlPc was converted into the hydroxyl derivative (HO-AlPc) by treatment with ammonium hydroxide and pyridine. Following the hydrolysis the substitution of the hydroxyl group with a fluorine group was affected using hydrofluoric acid.[15,28] In this paper we also illustrate a more straightforward and safer synthetic technique for acquiring F-AlPc along with more extensive physical characterization than currently available in the literature.

Experimental Section

Materials.

Potassium fluoride (KF, >99.0%) and sodium fluoride (NaF, >99.0%) were obtained from Sigma-Aldrich, dimethylsulfoxide (DMSO, 99.9%) was purchased from ACP, cesium fluoride (CsF, >99.0%) was purchased from Tokyo Chemical while all other solvents were purchased from Caledon Laboratories Ltd.. All chemicals and compounds were used as received unless otherwise specified. Chloro aluminum phthalocyanine (Cl-AlPc) was synthesized according to the literature,[28] and further purified by train sublimation prior to incorporation into devices. Bathocuproine (BCP 99.99%) from Sigma-Aldrich and Ag (99.99%) from R. D. Mathis Company were used as exciton blocking layers and cathode, respectively, and were also used as received. Fullerene (C_{60}, 99.5%) was purchased from SES Research and purified by train sublimation prior to incorporation into devices.

Synthesis of fluoro aluminum phthalocyanine (F-AlPc).

In a 50 mL three neck round-bottom flask with a reflux condenser and nitrogen inlet, Cl-AlPc (0.508 g, 0.883 mmol) and cesium fluoride (0.155 g, 1.02 mmol) were dissolved in DMSO (5 mL). The mixture was stirred and heated at 150 °C under nitrogen for 30 minutes. The crude product was allowed to cool to 130°C and was precipitated into 150 mL of isopropanol. The final product was gravity filtered resulting in a fine dark indigo powder. Yield 0.352g (71%). UV-vis (DMSO) λ_{max} = 671nm; HRMS [M+] calculated 558.1297, found 558.1277. Prior to device integration, F-AlPc was further purified by train sublimation to achieve electronic grade purity.

Characterization.

Ultraviolet−visible (UV−vis) spectroscopy was performed using PerkinElmer Lambda 1050 with a 10 mm quartz cuvette. Cyclic voltammetry was performed using a three-electrode cell assembly at room temperature in a 0.1M dichloromethane and tetrabutyl ammonium perchlorate (TBAP) electrolyte solution. The working electrode was a glassy carbon disk electrode, the counter electrode was a polished platinum wire and the reference electrode was Ag/AgCl. An internal standard of decamethyl ferrocene (bis(pentamethyl cyclopentadienyl)iron, Sigma-Aldrich). A scan rate was 100 mV/s was used for all measurements. The samples were bubbled using nitrogen until no dissolved oxygen was present (30-60 min prior to each run). Photoemission measurements were conducted on a PHI 5500 Multi-technique system using a monochromated Al Kα photon source (hν = 1,486.7 eV) for X-ray photoemission spectroscopy (XPS) and a non-monochromated He Iα photon source (hν = 21.22 eV) for UPS. Work function and valence-band measurements were carried out using UPS with the sample tilted to a take-off angle of 89° and under an applied bias of −15 V. The analysis chamber base pressure was $\approx 10^{-10}$ torr.

Device Fabrication.

All OPV devices were fabricated on commercially available patterned ITO substrates (Thin Film Device Inc. (TFD)) with a 145 nm ITO thickness and a sheet resistance of 15 Ω/□. Subsequent 5 min submerging in an ultrasonicating bath using detergent, distilled water, acetone and methanol was performed to clean the ITO substrates. Once dried by nitrogen, the ITO was treated with air plasma for 5 min to remove carbon residues. Post plasma treatment, a CHEMAT Technology KW-A4 spin coater was used to spin a layer of PEDOT:PSS (Clevios™ P VP AI 4083) at 500 rpm for 10 sec and 4000 rpm for 30 sec on the ITO substrate. The substrate was then heated at 110 °C for 15 min on a hot plate. The substrate was introduced into a custom built vacuum chamber where the devices were grown by thermal evaporation with a base pressure of $10x10^{-8}$ torr. The device structures consists of ITO/PEDOT:PSS/Active layer/BCP(8 nm)/Ag(80 nm), where the active layer and their respective thicknesses can be found in Table 2. Between growth of the BCP layer and the Ag cathode, devices were transferred from the vacuum chamber to nitrogen atmosphere glove box by means of antechamber, transfer arm and gate valve, to attach a shadow mask consisting of 5 active pixel area of 0.2 cm^2. Layer thickness and deposition rate were monitored using a quartz crystal microbalance (QCM). After the Ag layer was deposited, the OPV devices were transferred directly from the vacuum chamber back to the nitrogen atmosphere glove box. Silver paste (PELCO® Conductive Silver 187) was applied to the end Ag of electrode and ITO contact point to enhance electrical contact and left to cure for 30 minutes before testing. A 300 W ozone free xenon arc lamp with an air Mass 1.5 Global filter, fed through a Cornerstone™ 260 1/4 m monochromator and then into the glove box by way of a single branch liquid light guide was utilized as a solar simulator. The illumination levels for the test cell were kept at 100mW/cm^2. A UV-silicon photo-detector was used to calibrate the measurements. The current densities versus voltage (J–V) characteristics and external quantum efficiency were recorded, in the nitrogen atmosphere glove box, using a Keithley 2401 Low Voltage source meter controlled by a custom LabView program and a Newport Optical Power Meter 2936-R controlled by TracQ Basic software, respectively.

Results and Discussion

The synthesis of F-AlPc was accomplished by substitution of the chloride group with a fluoride group by simple heating of Cl-AlPc in a polar aprotic solvent such as dimethylformamide (DMF) or dimethyl sulfoxide (DMSO) in the presence of a fluoride salt such as cesium fluoride (CsF), potassium fluoride (KF) and sodium fluoride (NaF). In all cases the resulting product, F-AlPc, was obtained in high purity (> 99 %). The highest yield (≈ 70-80 %) was obtained when using the combination of DMSO and CsF. In any of the cases, F-AlPc was synthesized the need for incredibly dangerous chemicals such as hydrofluoric acid as has been previous described in the literature[15] (see experimental section for experimental details).

The effect of substitution of the chloride for the fluoride group on the AlPc was first characterized by UV-Vis spectroscopy. Both compounds were analysed in DMSO, chloroform and toluene solution as well as 40-50 nm solid films that were produced by thermal sublimation. **Figure 2** shows the characteristic scaled

absorbance of F-AlPc and Cl-AlPc in DMSO solution and as a solid film. As a comparison the effect of solvent on the absorbance of F-AlPc and Cl-AlPc, each in DMSO, chloroform and toluene can be found in **Table S1** in the supporting information. The optical band gap ($E_{Gap,Opt}$) and max absorbance (λ_{max}) were determined from the absorbance spectra and can be found in **Table 1**. The peak absorption of Cl-AlPc, in DMSO, occurs at λ_{max} = 680 nm while the peak absorption of F-AlPc is slightly blue shifted to λ_{max} = 671 nm (**Figure 2**). This small blue shift in absorbance corresponds to an increase in optical bang gap from $E_{Gap,Opt}$ =1.78 eV to $E_{g,opt}$ = 1.81 eV, for Cl-AlPc to F-AlPc respectively (**Table 1**). These results are consistent with the literature values for halo boron subphthalocyanines (BsubPcs), where little change was observed in the maximum absorbance of Cl-BsubPc and F-BsubPc, at 565 nm and 562 nm respectively.[14] What is interesting to note is that while the absorbance of the Cl-AlPc thin film has a red shift to 771 nm compared to its absorbance in DMSO solution, the absorbance of a F-AlPc thin film has a significant blue shift to 647 nm compared to its absorbance in DMSO solution. This observation of a blue-shift in the solid state compared to solution is rare and is likely attributable the unique linear stacked fluorine bridging morphology that F-AlPc is known to exhibit. This observation is consistent with the previously reported solid-sate absorption for F-AlPc.[29,30] There was no difference in the absorption properties of F-AlPc when CsF, KF or NaF was used for the synthesis of F-AlPc (**Figure S1**).

F-AlPc and Cl-AlPc were both characterized by cyclic voltammetry in dichloromethane solution. Characteristic electrochemical traces for both F-AlPc and Cl-AlPc can be found in **Figure S2**. F-AlPc had a lower oxidation peak potential, $E_{OX,\ peak}$ = +1.18 V and an increase in reduction peak potential, $E_{Red,\ peak}$ = -0.81 V compared to the Cl-AlPc ($E_{OX,\ peak}$ = +1.40 V and $E_{Red,\ peak}$ = -0.71 V, **Figure S2**). We previously reported a similar, but less significant, decrease in oxidation potential of 0.05 V between the Cl-BsubPc and F-BsubPc.[14] As a comparison, preliminary modelling was performed on F-AlPc and Cl-AlPc at the semi-empirical level using the PM3 parameter set in order to determine the effect of fluoride vs. chloride on the energy levels of the highest occupied molecular orbital (E_{HOMO}), lowest unoccupied molecular orbital (E_{LUMO}) and energy band gap ($E_{Gap,Opt}$). **Figure S3** compares the E_{LUMO} and E_{HOMO} obtained by preliminary modelling of both F-AlPc and Cl-AlPc. It appears that the substitution of a chloride group for a fluoride group resulted in an increase in E_{HOMO} and E_{LUMO} and $E_{Gap,Opt}$ of roughly 0.1 eV. This increase in simulated energy levels is much less than the difference in oxidation and reduction peaks observed by cyclic voltammetry but is still consistent.

Due to the relatively low solubility of both Cl-AlPc and F-AlPc a better estimate of E_{HOMO} energy levels of Cl-AlPc and F-AlPc was obtained by ultraviolet photoelectron spectroscopy (UPS) on thin films. The densities of states corresponding to the E_{HOMO} are represented by the peaks at lowest binding energy of the valence band spectra for each compound (**Figure S4**) and the corresponding ionization energies or E_{HOMO} and the work functions determined by UPS ($\boldsymbol{\Phi_{UPS}}$) and x-ray photoelectron spectroscopy ($\boldsymbol{\Phi_{XPS}}$) are tabulated in **Table 1**. The substitution of chloride for fluoride results in a significant change in $\boldsymbol{\Phi_{UPS}}$, $\boldsymbol{\Phi_{XPS}}$ and ultimately E_{HOMO}. For example, an increase of E_{HOMO} of as much as ≈1.0 eV was observed between Cl-AlPc (E_{HOMO} = -5.7 eV) and F-AlPc (E_{HOMO} = -4.7 eV). It is important to note that $\boldsymbol{\Phi_{UPS}} \approx \boldsymbol{\Phi_{XPS}}$, which confirms the obtained values. Having an estimation for the E_{HOMO} level and knowing the $E_{Gap,Opt}$ from the solid state absorbance of both AlPcs we then estimated the E_{LUMO}. In general, the transport energy gap, $E_{Gap,T}$, is equal to the $E_{Gap,Opt}$ plus the energy associate to the exciton binding E_{Ex} ($E_{Gap,T} = E_{Gap,Opt} + E_{Ex}$).[31] Cho *et al.* identified that for Cl-AlPc the E_{Ex} ≈ 0.24 eV, which gives an $E_{Gap,T}$ of around 1.9 eV *(when using* $E_{Gap,Opt}$ = 1.66 eV).[5] Therefore, assuming E_{Ex} ≈ 0.24 eV is similar for F-AlPc we can estimate E_{LUMO} levels by using the $E_{Gap,T}$ (**Table 1**). For comparison, **Figure 3** illustrates the E_{HOMO} calculated by UPS and the E_{LUMO} levels estimated from the $E_{Gap,T}$ for F-AlPc and Cl-AlPc and the literature values for C_{60}.

When making thin solid films of Cl-AlPc and F-AlPc we observed that under an identical setup F-AlPc would sublime at a much higher temperature (≈550 °C at 10^{-6} torr) compared to Cl-AlPc (≈400°C at 10^{-6} torr). Thereafter, simple thermo gravimetric analysis (TGA) was performed on synthetic crude samples of both Cl-AlPc and F-AlPc to study the mass loss with respect to the change in temperature. The corresponding TGA traces for the % mass loss and the scaled derivative of mass loss with respect to temperature can be found in **Figure S5**. The mass loss profile between Cl-AlPc and F-AlPc are significantly different. For example, F-AlPc shows no mass loss until roughly 625 °C (ambient pressure) while Cl-AlPc experiences significant mass loss at 550 °C (ambient pressure). The TGA profile and the elevated sublimation temperature for F-AlPc are consistent with its unique stacked fluorine-bridged AlPc organization.[15,16,32]

As previously mentioned, Cl-AlPc has already found application in OPV devices when paired with C_{60}.[5-9,33] Cl-AlPc and F-AlPc were therefore incorporated into PHJ OPV devices of varying architectures. Characteristic current versus voltage (I-V) plots as well as the external quantum efficiency (EQE) versus wavelength plots are illustrated in **Figure 4**. A baseline PHJ OPV device (device A) with a device architecture of ITO/PEDOT:PSS/Cl-AlPc(20 nm)/C_{60}(40 nm)/BCP (7.5 nm)/Ag(80 nm) was fabricated and characterized as having a short-circuit current density (J_{SC}) of 3.85 mA/cm^2, an open voltage circuit (V_{OC}) of 0.67 V, a fill factor (*FF*) of 0.48 and efficiency (η) of 1.23%. The electrical characteristics for this Cl-AlPc/C_{60} OPV device are similar to those reported in the literature[5-9,33] and are summarized in **Table 2**. Device B was fabricated with a similar architecture to device A except that Cl-AlPc was substituted for F-AlPc (ITO/PEDOT:PSS:PSS/F-AlPc(20 nm)/C_{60}(40 nm)/BCP(8 nm)/Ag(80 nm)). The use of F-AlPc resulted in a significant drop in V_{OC}, J_{SC} and *FF*. The drop in V_{OC} is not surprising due to the relatively high E_{HOMO} level of F-AlPc compared to Cl-AlPc (**Table 1, Table 2 & Figure 4**). The EQE plot (**Figure 4b**) shows a contribution to photo-generation at 620 nm, which corresponds to the absorption of F-AlPc (**Figure 2**), indicating that F-AlPc does however contribute to the photogeneration in the PHJ device. Many researchers have tried to investigate the dependence of V_{oc} value in OPV devices, until now it is still not well understood.[34,35] However, there is a suggestion that the maximum V_{oc} depends on the energy difference between the E_{HOMO} of the donor the E_{LUMO} of the acceptor at the interface in a PHJ device, which is also referred to as the interface gap (I_g).[36,37] As seen in **Figure 3**, I_g for Cl-AlPc/C_{60} is 1.4 V and for F-AlPc/C_{60} is 0.4 V, indicating that this reduction in I_g could be one of the main factor responsible for the reduction in V_{OC} (**Table 2**). The significant blue shift observed from the absorbance of F-AlPc compared to Cl-AlPc (**Figure 2**) allows for the absorption of photons at unique wavelengths previously unattainable using solely Cl-AlPc. Therefore, to show the potential for F-AlPc to compliment the absorption of Cl-AlPc, a ternary device was constructed with the following architecture ITO/PEDOT:PSS/F-AlPc(10 nm)/Cl-AlPc(10 nm)/C_{60}(40 nm)/BCP(8 nm)/Ag(80 nm) (device C). Compared to device A, the resulting devices were characterized by having a decrease in V_{OC} of 0.22 V and a modest increase in J_{SC} of 0.15

mA·cm^{-2} (**Figure 4**, **Table 2**). It is interesting to note that the EQE spectra for device C indicated a greater ratio of the AlPc peaks (600-800 nm) to C_{60} peaks (350-500 nm) compared to device A, which did not have any F-AlPc, indicating a more significant photo-generation when utilizing both Cl-AlPc and F-AlPc compared to just one or the other (**Figure 4**). This increase in photogeneration ratio between the AlPcs and C_{60} suggest that there are potentially two exciton-rectifying interfaces in this ternary device: the first between Cl-AlPc/C_{60} and the second between F-AlPc/Cl-AlPc.

An analysis of the respective E_{HOMO} and E_{LUMO} of F-AlPc and Cl-AlPc (**Figure 3**) indicates that the two could be paired within an OPV as an electron donor and electron acceptor respectively. Recently, Cl-AlPc was reported as an acceptor when paired with pentacene in a simple C_{60}-free PHJ OPV device.[38] In attempts to identify if our previous hypothesis regarding the two exciton-rectifying interfaces in this ternary device we decided to explore the concept of a C_{60}-free PHJ OPV device utilizing F-AlPc as a donor layer and Cl-AlPc as an acceptor layer in an all-AlPc device. Device D was constructed with the following architecture, ITO/PEDOT:PSS/F-AlPc(20 nm)/Cl-AlPc(40 nm)/BCP(7.5 nm)/Ag(80 nm) (**Figure 4, Table 3**). The resulting unoptimized device was characterized by having a V_{OC} = 0.37, $J_{SC=}$ 1.23 mA·cm^{-2}, FF = 0.24 and η_{Power} = 0.12 %. The resulting EQE spectrum corresponds to the merged absorption of Cl-AlPc and F-AlPc (**Figure 2** and **3**). These results further suggest that an exciton-rectifying interface does exist between F-AlPc and Cl-AlPc both in a ternary device as well as a simple bilayer PHJ OPV. While these electrical characteristics are below baseline they do represent the first all-AlPc OPV device, they confirm the uniqueness of F-AlPc and also confirm the potential use of Cl-AlPc as an electron acceptor in PHJ OPV devices.

Conclusions

In conclusion the facile synthesise of F-AlPc was accomplished by heating a DMF solution of Cl-AlPc in the presence of CsF, KF or NaF for less than an hour. This process circumvents the need to use highly toxic HF as a reagent. The resulting F-AlPc has a blue shift in peak absorbance of ≈ 8 nm in solution and ≈ 130 nm in the solid film compared to Cl-AlPc. These findings along with the substantial increase in sublimation temperature provides further evidence towards the unique linear stacked solid state arrangement of F-AlPc.

Electrochemical characterization of the Cl-AlPc and F-AlPc was also performed and a difference in oxidation potential ≈0.22 V between the two compounds was observed. UPS and XPS both identified that a significant change in work function and E_{HOMO} of as much as 1 eV also resulted from the substitution of fluoride for chloride.

Preliminary PHJ OPV devices were fabricated using thin layers of F-AlPc paired with C_{60}, ternary cells with both F-AlPc and Cl-AlPc paired with C_{60} and an all AlPc device where F-AlPc acted as the donor and Cl-AlPc acted as the acceptor. The EQE plots of the resulting devices illustrate that an exciton-rectifying interface is observed between the Cl-AlPc and F-AlPc layers in the ternary devices as well as the all AlPc device. These results further exemplify the use of AlPcs as candidates for PHJ OPV devices. While the previous studies regarding the chemical doping of F-AlPc have indicated that the doping process is not conducive to vacuum processing conditions the current efforts within our group are focused on doping of F-AlPc films and their incorporation into OPV devices.

Acknowledgements

The authors would like to acknowledge financial support from Saudi Basic Industries (SABIC). We would also like to acknowledge support from Natural Sciences and Engineer Research Council (NSERC) for a Banting Post-Doctoral fellowship to BHL and a Discovery Grant to TPB. This work was also supported by an Ontario Government Queen Elizabeth II Graduate Scholarship in Science and Technology (QEII-GSST) to RTW.

Notes

[a] University of Toronto, Dept. of Chemical Engineering & Applied Chemistry. 200 College Street, Toronto, Ontario M5S 3E5.

[b] University of Toronto, Dept. of Materials Science and Engineering. 200 College Street, Toronto, Ontario M5S 3E5.

[c] University of Toronto, Dept. of Chemistry. 80 St. George Street, Toronto, Ontario M5S 3H6.

* to whom correspondences should be addressed. E-mail: tim.bender@utoronto.ca

Electronic Supplementary Information (ESI) available: The absorbance, cyclic voltamatry, thermogravimetric and ultraviolet and x-ray photoluminescence spectroscopy discussion. See DOI: 10.1039/b000000x/

References

(1) McKeown, N. B. *Phthalocyanine Materials: Synthesis, Structure, and Function*; McKeown, N. B., Ed.; Cambridge University Press: Cambridge, United Kingdom, 1998.
(2) Dahlen, M. A. *Ind. Eng. Chem.* **1939**, *31*, 839–847.
(3) La Torre, De, G.; Vazquez, P.; Agullo-Lopez, F.; Torres, T. *J. Mater. Chem.* **1998**, *8*, 1671–1683.
(4) Claessens, C. G.; Hahn, U.; Torres, T. *Chem. Rec.* **2008**, *8*, 75–97.
(5) Cho, S. W.; Piper, L. F. J.; DeMasi, A.; Preston, A. R. H.; Smith, K. E.; Chauhan, K. V.; Sullivan, P.; Hatton, R. A.; Jones, T. S. *J. Phys. Chem. C* **2010**, *114*, 1928–1933.
(6) Chauhan, K. V.; Sullivan, P.; Yang, J. L.; Jones, T. S. *J. Phys. Chem. C* **2010**, *114*, 3304–3308.
(7) Chauhan, V.; Hatton, R.; Sullivan, P.; Jones, T.; Cho, S. W. *J. Mater. Chem.* **2009**, 1173–1178.
(8) Kim, D. Y.; So, F.; Gao, Y. *Sol. Energy Mater. Sol. Cells* **2009**, *93*, 1688–1691.
(9) Bailey-Salzman, R. F.; Rand, B. P.; Forrest, S. R. *Appl. Phys. Lett.* **2007**, *91*, 013508.
(10) Bamsey, N. M.; Yuen, A. P.; Hor, A.-M.; Klenkler, R.; Preston, J. S.; Loutfy, R. O. *Sol. Energy Mater. Sol. Cells* **2011**, *95*, 1970–1973.
(11) Morse, G. E.; Helander, M. G.; Maka, J. F.; Lu, Z.-H.; Bender, T. P. *ACS Appl. Mater. Interfaces* **2010**, *2*, 1934–1944.
(12) Castrucci, J. S.; Helander, M. G.; Morse, G. E.; Lu, Z.-H.; Yip, C. M.; Bender, T. P. *Cryst. Growth. Des.* **2012**, *12*, 1095–1100.
(13) Morse, G. E.; Helander, M. G.; Stanwick, J.; Sauks, J. M.; Paton, A. S.; Lu, Z.-H.; Bender, T. P. *J. Phys. Chem. C* **2011**, *115*, 11709–11718.
(14) Fulford, M. V.; Jaidka, D.; Paton, A. S.; Morse, G. E.; Brisson, E. R. L.; Lough, A. J.; Bender, T. P. *J. Chem. Eng. Data* **2012**, *57*, 2756–2765.
(15) Linsky, J. P.; Paul, T. R.; Nohr, R. S.; Kenney, M. E. *Inorg. Chem.* **1980**, *19*, 3131–3135.
(16) Kuznesof, P. M.; Wynne, K. J.; Nohr, R. S.; Kenney, M. E. *J. Chem. Soc., Chem. Commun.* **1980**, 121.
(17) Nohr, R. S.; Kuznesof, P. M.; Wynne, K. J.; Kenney, M. E.; Siebenman, P. G. *J. Amer. Chem. Soc.* **1981**, *103*, 4371–4377.
(18) Djurado, D.; Fabre, C.; Hamwi, A.; Cousseins, J. C. *Synth. Met.* **1987**, *22*, 121–128.
(19) Djurado, D.; Hamwi, A.; Fabre, C. *Synth. Met.* **1989**, *29*, 71–75.
(20) Wynne, K. J. *Inorg. Chem.* **1984**, *23*, 4658–4663.

(21) Djurado, D.; Fabre, C.; Hamwi, A.; Cousseins, J. C. *Mater. Res. Bull.* **1987**, *22*, 911–921.
(22) Djurado, D.; Hamwi, A.; Fabre, C.; Avignant, D.; Cousseins, J. C. *Synth. Met.* **1986**, *16*, 227–233.
(23) Djurado, D.; Fabre, C.; Hamwi, A.; Cousseins, J. C. *Synth. Met.* **1987**, *22*, 93–101.
(24) Berthet, G.; Djurado, D.; Fabre, C.; Faury, F.; Maleysson, C.; Robert, H. *Mol. Cryst. Liq. Cryst.* **1985**, *118*, 345–348.
(25) Berthet, G.; Blanc, J. P.; Germain, J. P.; Larbi, A.; Maleysson, C.; Robert, H. *Synth. Met.* **1987**, *18*, 715–720.
(26) Blanc, J. P.; Blasquez, G.; Germain, J. P.; Larbi, A.; Maleysson, C.; Robert, H. *Sens. Actuators* **1988**, *14*, 143–148.
(27) Passard, M.; Pauly, A.; Blanc, J. P.; Dogo, S.; Germain, J. P.; Maleysson, C. *Thin Solid Films* **1994**, *237*, 272–276.
(28) Guay, D.; Dodelet, J. P.; Cote, R.; Langford, C. H.; Gravel, D. *J. Electrochem. Soc.* **1989**, *136*, 2272–2280.
(29) Dann, A. J.; Fahy, M. R.; Jeynes, C.; Willis, M. R. *J. Phys. D: Appl. Phys.* **2000**, *19*, L217–L224.
(30) Hiromitsu, I.; Takeuchi, J.; Ito, T. *J. Phys. Soc. Jpn.* **1990**, *59*, 2922–2930.
(31) Hill, I. G.; Kahn, A.; Soos, Z. G.; Pascal, R. A., Jr. *Chem. Phys. Lett.* **2000**, *327*, 181–188.
(32) Djurado, D.; Hamwi, A.; Cousseins, J. C.; Bidar, H.; Fabre, C.; Berthet, G. *Synth. Met.* **1985**, *11*, 109–121.
(33) Williams, G.; Sutty, S.; Klenkler, R.; Aziz, H. *Sol. Energy Mater. Sol. Cells* **2014**, *124*, 217–226.
(34) Brabec, C. J.; Cravino, A.; Meissner, D.; Sariciftci, N. S. *Adv. Funct. Mater.* **2001**.
(35) Gledhill, S. E.; Scott, B.; Gregg, B. A. *J. Mater. Res.* **2005**, *20*, 3167–3179.
(36) Rand, B.; Burk, D.; Forrest, S. *Phys. Rev. B* **2007**, *75*, 115327–115311.
(37) Mutolo, K. L.; Mayo, E. I.; Rand, B. P.; Forrest, S. R.; Thompson, M. E. *J. Am. Chem. Soc* **2006**, *128*, 8108–8109.
(38) Beaumont, N. L. P.hD Thesis, The University of Warwick, 2013.

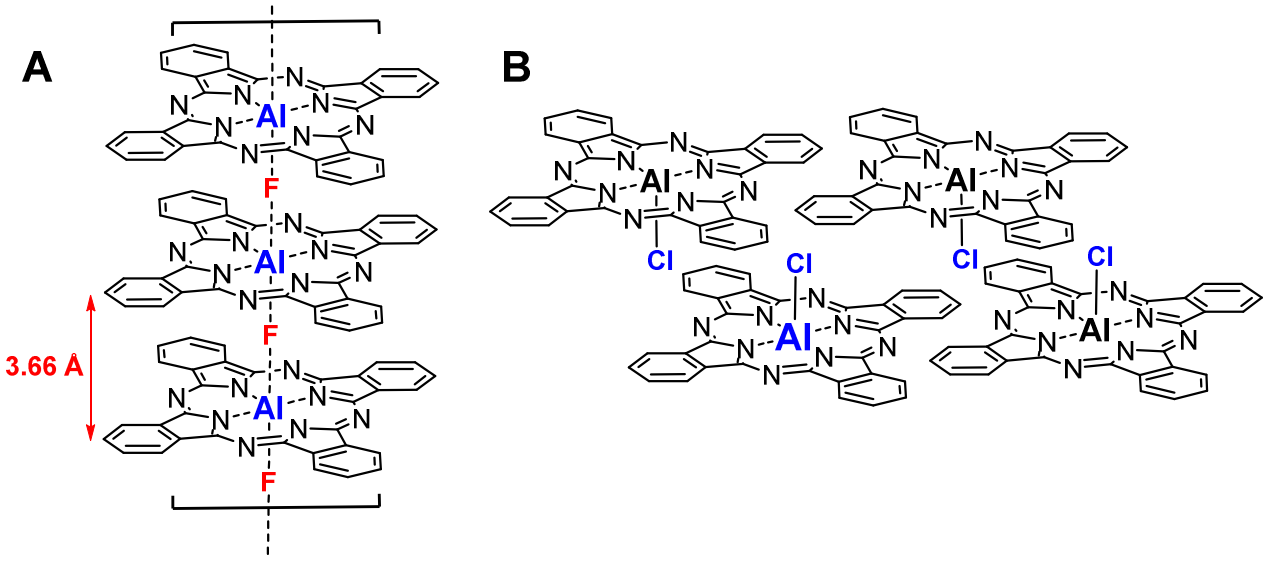

Figure 1. Molecular structure and schematic representation of the solid state arrangement of (A) F-AlPc and (B) Cl-AlPc.

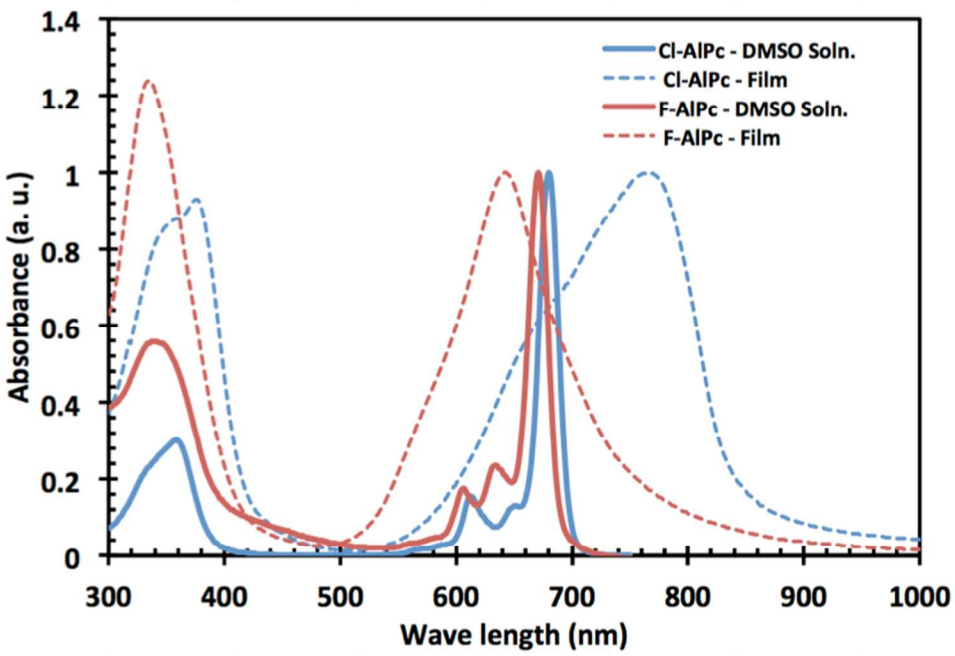

Figure 2.Normalized absorbance spectra of F-AlPc and Cl-AlPc in a DMSO solution and as a film.

Table 1. Physical characteristics of Cl-AlPc and F-AlPc.

Sample	λ_{MAX} (DMSO/Film)	$E_{Opt\ gap}$ (DMSO/Film)	Φ_{XPS}/ Φ_{UPS}	$E_{HOMO,UPS}$	E_{LUMO}[1]
	(nm)	(eV)	(eV)	(eV)	(eV)
Cl-AlPc	680 / 771	1.78 / 1.48	4.5 / 4.4	5.7	4.0
F-AlPc	671 / 647	1.81 / 1.61	3.6 / 3.6	4.7	2.9

[1] Calculated from: $E_{LUMO} = E_{HOMO,UPS} - E_{Opt\ gap} - E_{Ex}$ (where $E_{Ex} \approx 0.24$ eV).[5]

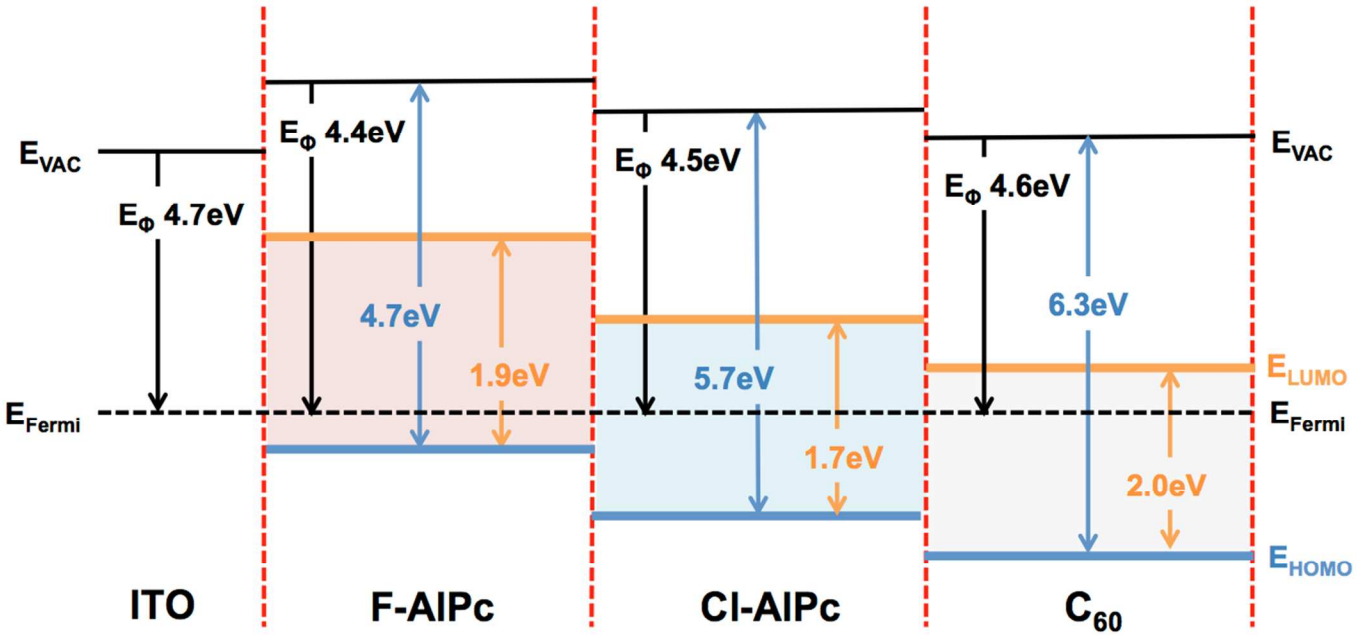

Figure 3. Schematic view of the E_{HOMO} levels and local vacuum level shifts for ITO/F-AlPc/Cl-AlPc/C_{60} heterojunctions. For comparison the Fermi energy levels were all assumed to be equal. The E_{HOMO} levels were obtained by UPS and the E_{LUMO} levels for Cl-AlPc and F-AlPc were estimated from the onset of the solid state UV-Vis absorbance (**Figure 2, Table 1**).

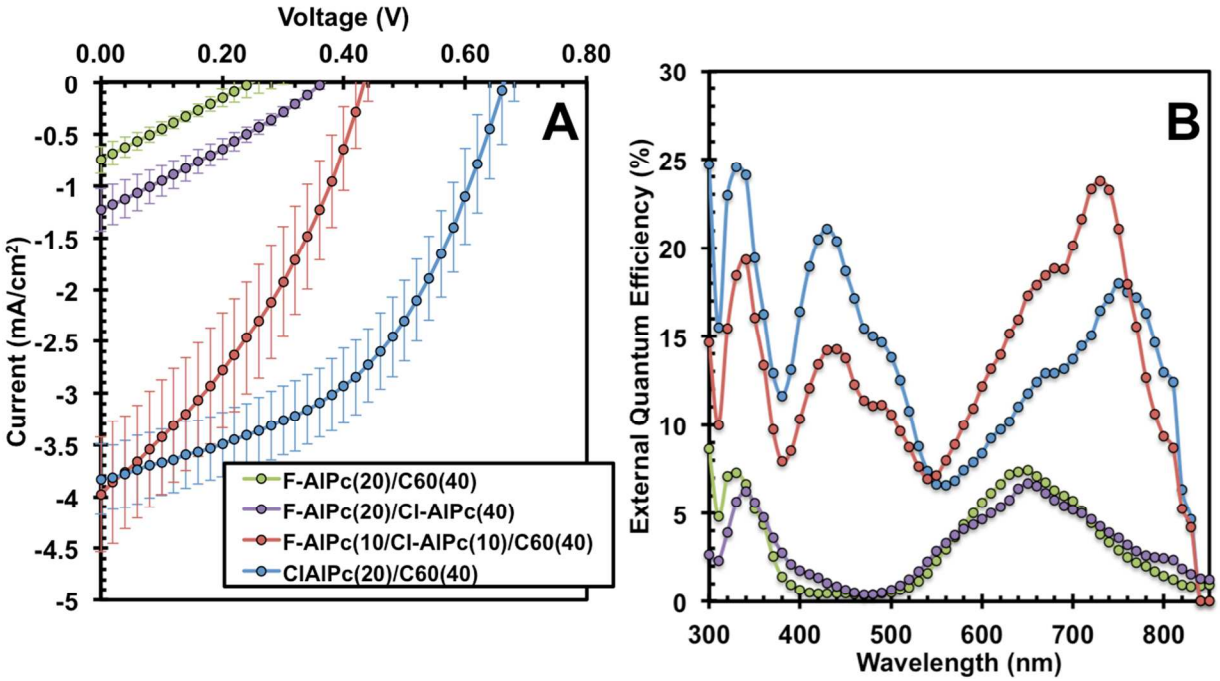

Figure 4. A) J-V curves and B) external quantum efficiency (EQE) for a series of F-AlPc / Cl-AlPc and C_{60} containing PHJ OPV devices. All devices were fabricated with the following structure: ITO/PEDOT:PSS/Active Layer/BCP(75 nm)/Ag(80 nm) where the active layer can be found in the legend in nm.

Table 2. Electrical characteristics of Cl-AlPc and F-AlPc containing PHJ OPV devices.

Device [a)]	*Active layer* (nm)	V_{OC} [b)] (V)	J_{SC} [b)] (mA·cm^{-2})	*FF* [b)]	η_{Power} [b)] (%)
A	Cl-AlPc (20nm)/C_{60} (40nm)	0.67±0.03	-3.85±0.3	0.48±0.03	1.23±0.17
B	F-AlPc(20nm)/C_{60}(40nm)	0.27±0.02	-0.7±0.07	0.24±0.02	0.05±0.006
C	F-AlPc(10nm)/Cl-AlPc(10nm)/C_{60}(40nm)	0.45±0.01	-4.0±0.5	0.34±0.03	0.61±0.1
D	F-AlPc(20nm)/ Cl-AlPc(40nm)	0.37±0.008	-1.23±0.2	0.28±0.01	0.13±0.02

[a)] Device structure: ITO/Pedot: PSS / (Active layer)/BCP(7.5nm)/Ag(80nm).
[b)] Devices characteristics taken from an average of 6-10 pixels over 2-4 devices.

For use in Table of content only

From Chloro to Fluoro, Expanding the Role of Aluminum Phthalocyanine in Organic Photovoltaic Devices.

*Benoît H. Lessard[1], Mohammad Al-Amar[1], Trevor M. Grant[1], Robin White[2], Zheng-Hong Lu[2] and Timothy P. Bender[1,2,3,]**

One sentence description for TOC:

Fluoro aluminum phthalocyanine (F-AlPc) was synthesized, characterized and its potential was assessed as a donor molecule for planar heterojunction organic photovoltaic devices.